European Journal of Pharmaceutics and Biopharmaceutics 136 (2019) 108–119

Contents lists available at ScienceDirect

European Journal of Pharmaceutics and Biopharmaceutics

journal homepage: www.elsevier.com/locate/ejpb

Research paper

Development of electrospun nanofibers that enable high loading and long-term viability of probiotics

Katja Škrlec[a,b,1], Špela Zupančič[c,1], Sonja Prpar Mihevc[a], Petra Kocbek[c], Julijana Kristl[c,*], Aleš Berlec[a,c,*]

[a] Department of Biotechnology, Jožef Stefan Institute, Jamova 39, SI-1000 Ljubljana, Slovenia
[b] Graduate School of Biomedicine, Faculty of Medicine, University of Ljubljana, Vrazov trg 2, SI-1000 Ljubljana, Slovenia
[c] Faculty of Pharmacy, University of Ljubljana, Aškerčeva 7, SI-1000 Ljubljana, Slovenia

ARTICLE INFO

Keywords:
Nanotechnology
Biotechnology
Probiotics
Lactobacillus
Electrospinning
Nanofibers
Process optimization
Solid formulation
Stability
Local delivery

ABSTRACT

The interest in probiotics has grown in recent years due to increased awareness of the importance of microbiota for human health. We present the development of monolithic poly(ethylene oxide) and composite poly(ethylene oxide)/lyoprotectant nanofibers loaded with the probiotic *Lactobacillus plantarum* ATCC 8014. High loading was achieved for *L. plantarum* cells (up to 7.6×10^8 colony-forming unit/mg) that were either unmodified or expressing mCherry fluorescent protein. The initial concentration of *L. plantarum* in poly(ethylene oxide) solution was reported, for the first time, as the most critical parameter for its high viability after electrospinning, whereas the applied electric voltage and relative humidity during electrospinning did not vitally impact upon *L. plantarum* viability. The presence of amorphous lyoprotectant (especially trehalose) in the nanofibers promoted *L. plantarum* survival due to lyoprotectant interactions with *L. plantarum* cells. *L. plantarum* cells in nanofibers were stable over 24 weeks at low temperature, thereby achieving stability comparable with that in lyophilizates. The poly(ethylene oxide) nanofibers released almost all of the *L. plantarum* cells over 30 min, which will be adequate for their local administration. Our integrated approach enabled development of a promising nanodelivery system that provides high loading and long-term viability of *L. plantarum* in nanofibers, for local delivery to re-establish the microbiota balance e.g. in vagina.

1. Introduction

The growing knowledge about human microbiota has increased awareness of the importance of microbe–host interactions for human health [1]. An imbalance in the composition of the human microbiota can cause pathologies that are collectively known as 'dysbioses', and include inflammatory bowel disease [2], irritable bowel syndrome [3], bacterial vaginosis [4], periodontitis [5], and skin diseases [6]. In dysbiosis, the relationship between the microbiota, their metabolic products, and the host immune system is disrupted. The microbial balance can be restored by addition of sufficient quantities of beneficial bacteria; i.e., probiotics [7].

The currently used probiotics are mostly lactic acid bacteria, and are most commonly from non-spore forming genus *Lactobacillus* [8]. *Lactobacillus plantarum* is a highly investigated species, with several hundred strains that have had their genome sequenced. Among these, *L. plantarum* 299v and *L. plantarum* WCFS1 have been the most studied, and are clinically effective for prevention and treatment of gastrointestinal disorders, including ulcerative colitis and irritable bowel syndrome [9–12]. *L. plantarum* ATCC 10241 has shown potential as a therapeutic agent to both prevent burn wound infection and alleviate wound scarring [13]. Also, apart from this intrinsic probiotic effect, *L. plantarum* can be genetically engineered for the production of a wide range of therapeutic and prophylactic proteins [14].

To administer a sufficient dose of viable probiotics, an appropriate delivery system is required. The delivery system needs to be patient-friendly, to provide effective local delivery, to incorporate large quantities of viable probiotic bacteria, and to guarantee long-term stability

Abbreviations: ANOVA, one-way analysis of variance; CFU, colony-forming unit; DSC, differential scanning calorimetry; FTIR, Fourier transform infrared; MRS, De Man, Rogosa and Sharpe; PBS, phoshate-buffered saline; PEO, poly(ethylene oxide); SD, standard deviation; SEM, scanning electron microscopy

* Corresponding authors at: Faculty of Pharmacy, University of Ljubljana, Aškerčeva 7, SI-1000 Ljubljana, Slovenia (J. Kristl). Department of Biotechnology, Jožef Stefan Institute, Jamova 39, SI-1000 Ljubljana, Slovenia (A. Berlec).
E-mail addresses: julijana.kristl@ffa.uni-lj.si (J. Kristl), ales.berlec@ijs.si (A. Berlec).
[1] These authors contributed equally.

https://doi.org/10.1016/j.ejpb.2019.01.013
Received 20 November 2018; Received in revised form 11 January 2019; Accepted 15 January 2019
Available online 17 January 2019
0939-6411/

of the probiotics, preferably at room temperature. Long-term stability can be achieved by transforming probiotics from aqueous dispersions to dry forms using a suitable drying process, such as spray-drying, lyophilization, vacuum drying, and fluidized bed drying [15,16]. Lyoprotectants are also usually added to promote the viability of the probiotics [17,18]. Drying also reduces the weight of any formulation and the space required for its storage, which facilitates handling of probiotic cells and allows controlled dosing [19]. Currently, lyophilization and spray-drying have been the most studied [15]; however, the applicability for local use of such powdered formulations that are obtained after drying is limited, although it was recently improved by pressing into tablets and film coating [20]. Instead, electrospinning is emerging as an attractive alternative method that enables drying of probiotics and preparation of a solid dosage form in a single step [21].

Electrospinning techniques enable the production of nanofibers from electrostatically driven jets of polymer solutions. The diameters of the fibers obtained range between tens of nanometers (i.e., nanofibers) to a few micrometers. Nanofibers can be used in wound dressings, as drug delivery systems, and as three-dimensional scaffolds for bone and tissue regeneration [5,22–25]. They have mostly been investigated for delivery of small drug molecules, which have included: antibacterials or antifungal agents (e.g., for treating of bacterial vaginosis, candidiasis, other genital infections [26,27], periodontal disease [28]), anticancer agents (e.g. for local chemotherapies [29]), antioxidants, and anti-inflammatory agents [30], as well as proteins, such as enzymes [31].

Recently, electrospinning was introduced as a new method for incorporation of microbial cells into nanofibers [32]. *Lactobacillus acidophilus* was incorporated into agrowaste-based nanofibers [33], and *Bifidobacterium animalis* subsp. *lactis* Bb12 into poly(vinyl alcohol) electrospun fibers [34]. Nonprobiotic bacteria (e.g., *Escherichia coli, Staphylococcus epidermidis*) and bacterial viruses (e.g., T7, T4, λ) have been encapsulated into poly(vinyl alcohol) based nanofibers, although they showed low viability following this incorporation process [35]. Although electrospinning has been shown to be a promising process for probiotic incorporation [36], the effects of the process, solutions and environment parameters on probiotic viability are still poorly understood due to a lack of studies in this field.

Therefore, the present study was designed to investigate electrospinning further, as a method to incorporate *L. plantarum* ATCC 8014 into monolithic poly(ethylene oxide) (PEO) and composite PEO/ lyoprotectant nanofibers. PEO was chosen as it is a biocompatible, mucoadhesive, and water-soluble polymer that appears not to interfere with the bioactivity of delivered substances [37], along with lyoprotectants (i.e., sucrose, trehalose) as molecules that are known to help to preserve the viability of probiotics during their drying [38]. To date, the use of lyoprotectants has not been explored in any detail for electrospinning. The particular focus here was thus to initially determine the effects on bacterial viability of: (i) the electrospinning process (i.e., applied voltage); (ii) the environment (i.e., relative humidity); and (iii) the solution parameters (i.e., *L. plantarum* cell concentration, lyoprotectant in the polymer solution). Furthermore, we aimed to determine the optimal parameters here that would provide the production of nanofibers with high loads of viable *L. plantarum* that are associated with their long-term stability during storage, as these represent the two crucial properties in the design of promising formulations. In addition, the effects of *L. plantarum* on the nanofiber morphology, the solid state of the excipients, and the interactions between all of the components were investigated, to better understand the probiotic viability in these formulations.

2. Materials and methods

2.1. Materials

PEO (M_w, 900 kDa), sucrose and chloramphenicol were from Sigma Aldrich (Germany). Trehalose dihydrate was from Calbiochem (Merck, Germany) and phosphate buffered saline (PBS; pH 7.4; osmolality: 280–315 mOsm/kg) from Gibco (Life Technologies, USA). De Man, Rogosa and Sharpe (MRS) medium for culturing of *L. plantarum* was from Merck (Germany).

2.2. Culturing of L. plantarum

Lactobacillus plantarum ATCC 8014 was grown at 37 °C in MRS medium without aeration, or on MRS medium solidified with 1.5% agar. For long-term storage, the *L. plantarum* was kept frozen at −80 °C in MRS with 20% glycerol. For each experiment, fresh bacterial cell cultures were cultivated as follows: a frozen culture of *L. plantarum* was transferred onto a MRS agar plate and incubated for 2 days at 37 °C. A single colony of *L. plantarum* was picked from the plate, inoculated into 10 mL MRS medium, and incubated at 37 °C for 24 h. Overnight cultures were diluted (1:100, v/v) in fresh MRS medium and grown for 16 h, which was the time that was experimentally determined as that at which *L. plantarum* reached stationary growth phase. The cultures were centrifuged at 5000*g* for 10 min (Sorvall Lynx 4000; ThermoFisher Scientific, USA). The cells were then washed twice with PBS and resuspended in an appropriate volume of sterile water, to obtain concentrations of bacteria from 10^9 to 10^{12} colony-forming units (CFU)/mL.

2.3. Engineering of L. plantarum to produce the fluorescent protein mCherry

Electroporation of *L. plantarum* was performed according to Berthier et al. [39], using a Gene Pulser II apparatus (Bio-Rad, USA) and the pCDLbu-1ΔEc_Ptuf34_mCherry plasmid [40] that encodes the gene for fluorescent protein mCherry under the control of the strong P_{tuf} promoter. *L. plantarum* with the pCDLbu-1ΔEc_Ptuf34_mCherry plasmid were grown as described above, with the exception that the MRS was supplemented with 10 μg/mL chloramphenicol. This plasmid provided continuous expression of mCherry, and thus fluorescence detection of these cells.

2.4. Preparation and characterization of PEO solutions containing L. plantarum

PEO powder (4% w/v) was added to an aqueous dispersion of *L. plantarum*, and these were stirred for 4 h at 25 °C prior to the electrospinning. To prepare nanofibers with lyoprotectants, sucrose or trehalose dihydrate (4% (w/v)) were added into the *L. plantarum* dispersions in PEO solution, which contained 10^{12} CFU/mL *L. plantarum*.

The conductivities of the 4% (w/v) PEO solutions without and with *L. plantarum* (10^{12} CFU/mL) were determined at 25 °C (MC226 conductivity meter and electrode; Inlab 741, Mettler Toledo, Switzerland). The viscosity measurements of the 4% (w/v) PEO solutions without and with *L. plantarum* (10^{12} CFU/mL) were performed using a cone-plate measuring system (CP50-2; cone radius, 24.981 mm; cone angle, 2.001°; sample volume, 1.15 mL) with a rheometer (Physica MCR 301; Anton Paar, Graz, Austria) at a constant temperature of 25.0 ± 0.1 °C in rotational mode, for shear rates between 1 s^{-1} and 100 s^{-1}. The data for the viscosities at the shear rate of 2 s^{-1} are presented.

2.5. Preparation of electrospun nanofibers

To obtain nanofibers, 4% (w/v) PEO solutions without and with *L. plantarum* (and without and with lyoprotectants) were loaded into 5 mL syringes fitted with a metal needle (inner diameter, 1 mm), which was mounted horizontally on a syringe pump (model R-99E; RazelTM, Linari Engineering s.r.L., Italy). The electrode of a high-voltage power supply (model HVG-P60-R-EU; Linari Engineering s.r.L., Italy) was clamped to the metal needle, and the collector was grounded and covered with aluminum foil. The process used a flow rate of 0.4 mL/h, voltage of 15 kV, and nozzle-to-collector distance of 15 cm. The

environmental temperature was 24 ± 2 °C, with the relative humidity controlled at 20%, 35%, or 55%. To evaluate the effects of the applied voltage on the *L. plantarum* viability, 4% (w/v) PEO dispersions with 10^{12} CFU/mL *L. plantarum* cells were also electrospun at 10 kV with a flow rate of 0.2 mL/h, and 20 kV with a flow rate of 0.5 mL/h, at 24 ± 2 °C and relative humidity 20% ± 2%.

2.6. Lyophilization of L. plantarum dispersions

The dispersions of *L. plantarum* (10^{12} CFU/mL) were prepared and lyophilized (Chris Beta 1–8 K; Martin Chris, Germany), using sterile water and using 4% (w/v) PEO without and with 4% (w/v) sucrose or 4% (w/v) trehalose dihydrate. These dispersions were frozen at −80 °C, and then the primary drying was performed at shelf temperature, T_{shelf}, of –5 °C and pressure of 0.63 mbar for 24 h, with the secondary drying at T_{shelf} of 20 °C for 1 h.

2.7. Characterization of nanofiber morphology

The nanofibers were attached to metal stubs with double-sided conductive tape (diameter, 12 mm; Oxford Instruments, Oxon, UK) and 3 μL of each dispersion with *L. plantarum* was pipetted onto the metal stub and air dried. These samples were examined under scanning electron microscope (SEM; Supra 35 VP; Carl Zeiss, Oberkochen, Germany), that allowed a high-resolution imaging of the non-coated samples at low accelerating voltage (1 kV) using a secondary detector with negligible electrical surface charging. The diameters of 50 randomly selected nanofibers were measured using the ImageJ 1.44p software (National Institutes of Health, USA) to determine the mean nanofiber diameter. The diameters of the *L. plantarum*-loaded nanofibers were measured at places without cells. To evaluate the number of *L. plantarum* cells on the upper layer of the nanofiber mats, the cells were counted on the images acquired at five different positions on the nanofiber mat, at 6.000× magnification.

Nanofibers with *L. plantarum* that produced mCherry were electrospun onto glass slides, which were examined under confocal microscope (LSM 710; Carl Zeiss, Oberkochen, Germany). The mCherry was excited with an argon laser (at 587 nm) and the emission was filtered with a narrow-band 610-nm filter. All of the images were taken under the same settings and were analyzed using the ZEN lite 2012 software (Carl Zeiss, Oberkochen, Germany).

2.8. Thermal analysis of nanofibers

Differential scanning calorimetry (DSC; Mettler Toledo, Switzerland) was used to evaluate the crystallinity of the pure PEO, sucrose, and trehalose dihydrate powders, the lyophilized *L. plantarum,* and of the physical mixtures of PEO with sucrose or trehalose dihydrate (1:1, w/w), the nanofibers of PEO without and with sucrose or trehalose dihydrate (1:1, w/w), and *L. plantarum*-loaded nanofibers of PEO without and with sucrose or trehalose dihydrate (1:1, w/w). These measurements were performed using ~ 5 mg samples, which were weighed in aluminum pans with a pin hole. The heating rate was 10 °C/min, and the nitrogen purge rate was 50 mL/min. All of the samples were analyzed in the temperature range from 0 °C to 220 °C, and the DSC curves obtained were normalized to the sample mass.

The moisture content of the pure substances and the physical mixtures of PEO and the lyoprotectants (1:1, w/w) were determined for all of the nanofiber samples using thermogravimetric analysis (TGA; Mettler Toledo, Switzerland). Measurements were carried out between 30 °C and 220 °C, with a heating rate of 10 °C/min, under a constant nitrogen flow rate of 50 mL/min. The initial sample mass was ~5 mg.

2.9. Fourier transform infrared spectroscopy

The Fourier transform infrared (FTIR) spectra of the pure substances, the physical mixtures of PEO and the lyoprotectants (1:1, w/w), and all of the nanofiber samples were recorded using a FTIR spectrometer with an attenuated total reflectance accessory (Nexus, Thermo Nicolet, Madison, USA). FTIR spectroscopy was carried out at a resolution of 2 cm^{-1}, with 32 scans from 600 cm^{-1} to 4000 cm^{-1}.

2.10. Viability of L. plantarum in PEO solutions, nanofibers, and lyophilizates

The viabilities of the *L. plantarum* cells in PEO solutions, nanofibers and lyophilizates were determined using the drop-plate method [41]. Briefly, serial ten-fold dilutions were prepared in PBS from *L. plantarum*-containing polymer solutions, from dispersion of known amounts of *L. plantarum*-loaded nanofibers, and from dispersion of *L. plantarum* lyophilizates. Five 10 μL drops of each dilution were pipetted onto an agar plate and incubated at 37 °C for 2 days. Only the dilutions that produced 3 to 30 colonies per drop were counted. These data are expressed as CFU/mL for *L. plantarum* in the dispersions, and as CFU/mg for *L. plantarum* in the nanofibers and lyophilizates.

The experimentally determined loading of *L. plantarum* was compared to their theoretically determined loading. The theoretical loading was calculated as the number of *L. plantarum* cells in the polymer solution (CFU) per dry weight of polymer, *L. plantarum* cells, and lyoprotectants in 1 mL dispersion. The mass of 10^{10} dry *L. plantarum* cells was assumed to be 0.54 mg (based on weights of bacterial lyophilizates obtained from bacterial dispersions in sterile water).

2.11. Long-term storage of L. plantarum in nanofibers and lyophilizates

Defined masses of nanofibers and lyophilizates were stored in desiccators at 4 °C or 25 °C at the constant relative humidity of 11% (maintained using a saturated solution of LiCl). The viability of the *L. plantarum* in nanofibers and lyophilizates was analyzed at predefined times (nanofibers, after 1, 3, 8, 12, 24 weeks; lyophilizates, after 3, 24 weeks), as described in Section 2.10.

2.12. Release of L. plantarum from nanofibers

L. plantarum-loaded PEO nanofibers (100 mg) were added to 20 mL vials that contained 10 mL PBS as the release medium. The samples were stirred at 50 rpm. At predefined times (5, 10, 15, 20, 25, 30, 40, 50, 60, 70, 90 min), 100 μL of each sample was withdrawn and replenished with fresh PBS. These samples were diluted with 900 μL PBS, and the release of *L. plantarum* was determined by two independent and complementary methods: the drop-plate method (Section 2.10), where the CFU were determined; and the measurement of fluorescence of *L. plantarum* that expressed the fluorescent protein mCherry. For mCherry-expressing *L. plantarum*, the samples were diluted 1:10 in PBS, and 200 μL of these dilutions was transferred into black flat-bottomed 96-well plates (Corning, USA). The fluorescence was measured using a microplate reader (Infinite M1000; Tecan, Switzerland) with excitation/ emission at 587/610 nm. The data obtained by both of these methods are presented as the cumulative release of *L. plantarum* with time. The *L. plantarum* release from the nanofibers was measured in triplicates.

2.13. Statistical analysis

The effects of the process parameters and solution compositions on nanofiber diameters and *L. plantarum* viability were analyzed statistically by applying one-way analysis of variance (ANOVA) with Tukey's *post-hoc* tests (*, $\alpha < 0.05$; **, $\alpha < 0.01$; ***, $\alpha < 0.001$) using the OriginPro 2017 software (OriginLab Corporation, USA). All of the data are presented as means ± standard deviation (SD).

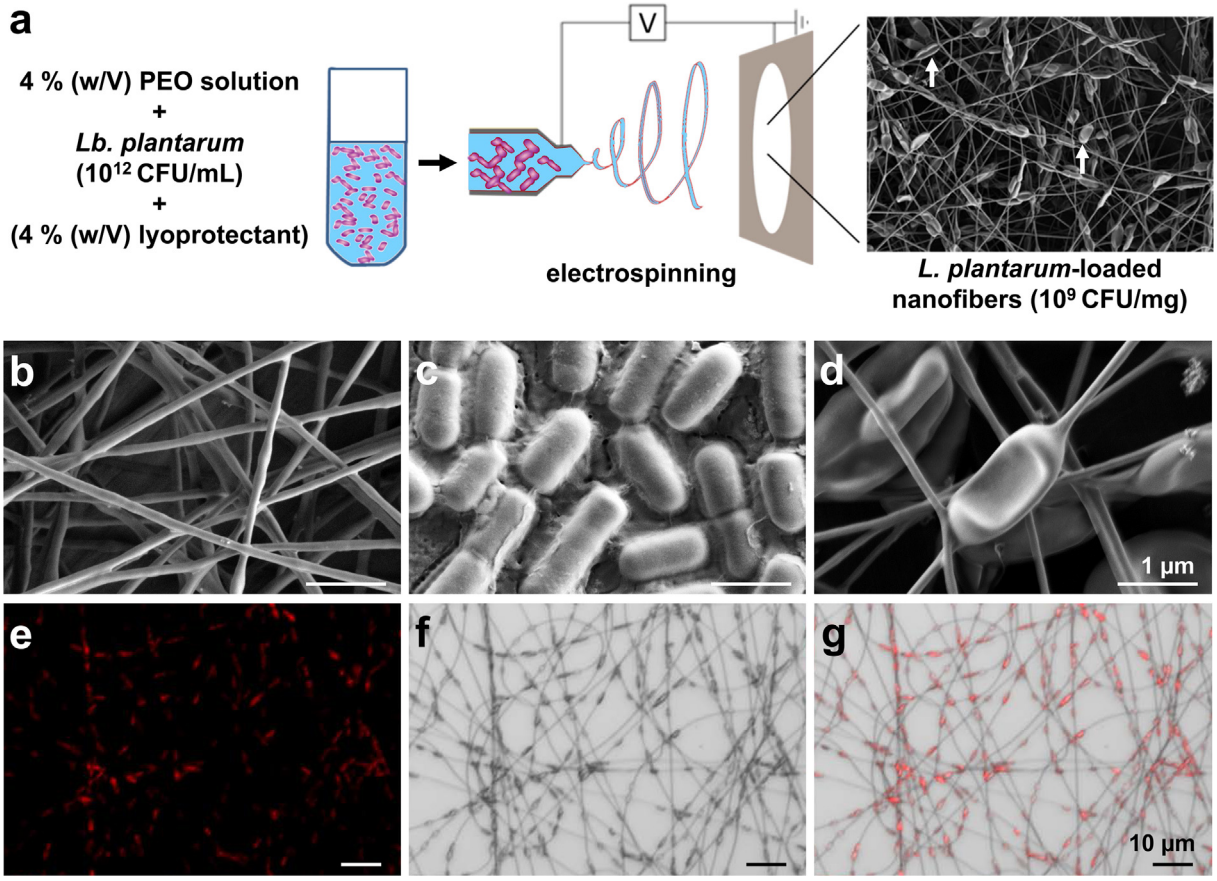

Fig. 1. **(a)** Schematic representation of electrospinning of poly(ethylene oxide) (PEO) without and with lyoprotectants and with *L. plantarum*, for the preparation of *L. plantarum*-loaded nanofibers. Arrows indicate individual and dividing cells in the nanofibers. Scanning electron microscopy images are shown for (**b**) pure PEO nanofibers, (**c**) *L. plantarum* cells air dried from water dispersion and (**d**) *L. plantarum*-loaded PEO nanofibers. Confocal microscopy images are also shown for PEO nanofibers with incorporated *L. plantarum* cells that harbor the pCDLbu-1ΔEc_Ptuf34_mCherry plasmid, as (**e**) fluorescence, (**f**) bright-field, and (**g**) merged images.

3. Results and discussion

3.1. Incorporation of L. plantarum cells into PEO nanofibers

Electrospinning is a promising process for formulation of nanofibers and their incorporation of probiotics (Fig. 1a). The nanofibers from the mucoadhesive PEO without *L. plantarum* were uniform and beadless, with mean diameter of 135 ± 25 nm (Fig. 1b). Local thickenings in the nanofibers indicated successful incorporation of the probiotic *L. plantarum* (Fig. 1c) into the PEO nanofibers (Fig. 1d). Although the *L. plantarum* cells had a greater diameter (492 ± 35 nm) than the nanofibers, they were entirely coated with polymer and thus enclosed within the nanofibers. The *L. plantarum* cells were oriented along the nanofibers, which is in line with the study of Salalha et al. (2006), who showed that randomly oriented bacteria in a polymer solution start to orient during the electrospinning in the Taylor cone mainly along the stream lines, and that these further align in the jet, which at the end solidifies into the nanofibers [42]. The *L. plantarum* in the nanofibers were incorporated as individual or dividing cells, with even distributions in the nanofiber mats, as observed by both SEM (Fig. 1a, d) and fluorescence microscopy (Fig. 1e-g). The *L. plantarum* cells that produced mCherry were seen as bright red fluorescent rods within thickenings of the PEO nanofibers. The *L. plantarum* incorporated into the nanofibers showed a flattened morphology (Fig. 1d) in comparison to those air dried from dispersions (Fig. 1c). The diameter of the *L. plantarum* cells incorporated into the nanofibers was 815 ± 115 nm, which was thicker than the air-dried *L. plantarum* alone or with additional theoretical PEO layer. The noticeably changed morphology of the *L. plantarum* might have been the consequence of their drying and dehydration and/ or the mechanical stress they had undergone [42,43].

3.2. The process parameters and solution compositions influence nanofiber morphology

Nanofiber morphology can be influenced by several parameters [44], among which those investigated here were: (i) the process parameter of applied voltage; (ii) the environmental parameter of relative humidity; and (iii) the solution parameters of concentration of *L. plantarum* cells and addition of lyoprotectants into the polymer solution.

The applied voltage was from 10 kV to 20 kV and did not significantly affect the thickness of the nanofibers produced (Fig. 2a). This is contrary to the study of Beachley and Wen [45], who reported significant decreases in nanofiber diameters with increasing applied voltage across the same range. In the present study, the uniformity of the nanofiber diameters was probably due to the adjustment of two parameters at the same time, as the increase in applied voltage was accompanied by an increased flow rate; this was necessary, as otherwise the solution would either drip at 10 kV or be dried on the nozzle at 20 kV.

The higher relative humidity resulted in a significant decrease in the nanofiber diameters (Fig. 2a), which is in line with our previous report [46]. At 55% relative humidity, electrospun nanofibers were the thinnest (diameter, 81 ± 18 nm), which resulted in a beaded morphology that was not the consequence of incorporated *L. plantarum*. On the other hand, the incorporation of the lyoprotectants (sucrose, trehalose) had no significant effects on the fiber diameters (Fig. 2b).

Increased concentrations of *L. plantarum* cells in the PEO solution

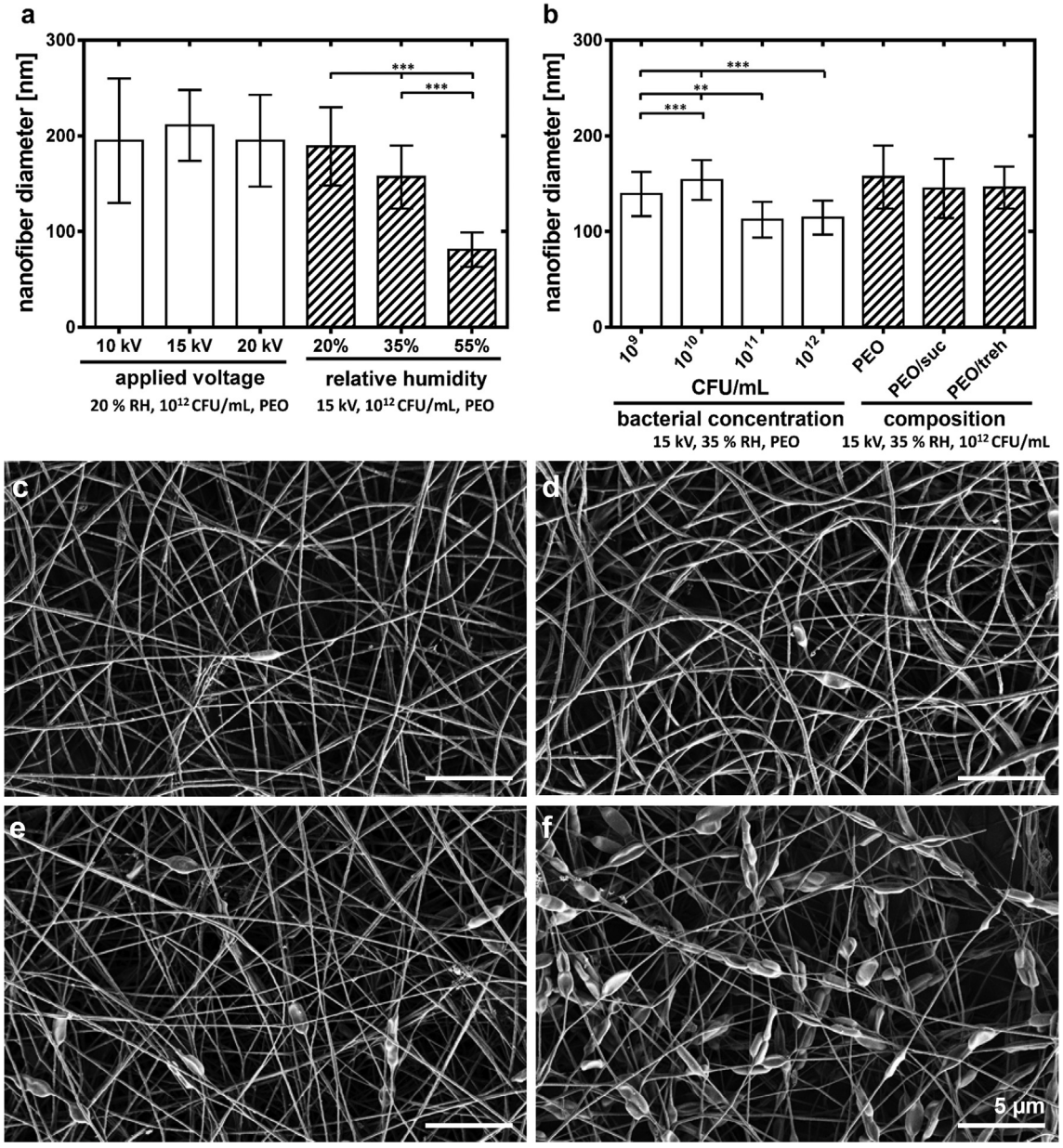

Fig. 2. Effects of the process and environmental parameters (i.e., the applied voltage and relative humidity) (**a**), and the properties of the polymer solution (i.e, *L. plantarum* concentrations and addition of lyoprotectants) (**b**) on the diameters of the *L. plantarum*-loaded nanofibers. Scanning electron microscopy images are also shown for *L. plantarum*-loaded poly(ethylene oxide) (PEO) nanofibers prepared from PEO solutions with different *L. plantarum* concentrations: 10^9 CFU/mL (**c**); 10^{10} CFU/mL (**d**); 10^{11} CFU/mL (**e**); and 10^{12} CFU/mL (**f**). **, $\alpha < 0.01$; ***, $\alpha < 0.001$; RH, relative humidity.

resulted in proportional increases in the numbers of incorporated cells, as observed for the upper layer of the nanofiber mats (Fig. 2c-f). The polymer solution with 10^{12} CFU/mL *L. plantarum* resulted in 184.9 ± 4.0 cells per 1000 µm^2 nanofiber mat surface, with 10^{11} CFU/mL resulting in 29 ± 4.4 cells, 10^{10} CFU/mL in 4.0 ± 0.8 cells, and 10^9 CFU/mL in 0.4 ± 0.7 cells, all per 1000 µm^2 and based on the analysis of the SEM images. Increasing the concentrations of the *L. plantarum* cells to above 10^{11} CFU/mL also resulted in significant decreases in the nanofiber diameters (Fig. 2b). The addition of the *L. plantarum* to the PEO solutions changed the dispersion conductivity and viscosity, due to the extracellular proteins and ions introduced with the probiotics or with the culture medium that remained after centrifugation. For example, addition of ~10^{12} CFU/mL of *L. plantarum* into the polymer solution increased the conductivity from 2.0 mS/cm to 4.8 mS/cm, and the viscosity of the dispersion from 1360 mPas to 1710 mPas. Increased conductivity and viscosity have been reported to influence nanofiber diameters in opposing ways, as decreased and increased nanofiber diameters, respectively [44,47,48]. In the present study, the decreased nanofiber diameters seen can be attributed to the more prominent influence of conductivity over viscosity (Fig. 2b).

To increase the *L. plantarum* viability in the nanofibers, each of two lyoprotectants (i.e., sucrose, trehalose) were added to the PEO solutions, from which composite nanofibers were successfully prepared that showed high lyoprotectant levels (PEO:lyoprotectant, 1:1 (w/w)). In other studies, the proportion of polymer to lyoprotectant was 3:1 (w/w) [49,50]. However, their mean nanofibers diameters were ~ 150 nm, and these were not significantly larger than those of the PEO nanofibers without the lyoprotectants in the present study (135 nm). The SEM images of the PEO/sucrose and PEO/trehalose nanofibers without or with *L. plantarum* showed formation of multiple 'necks' (Fig. 3). These necks were not evenly spaced along the nanofibers, and they had diameters of ~45 nm. Additionally, thin fibrillar structures with diameters

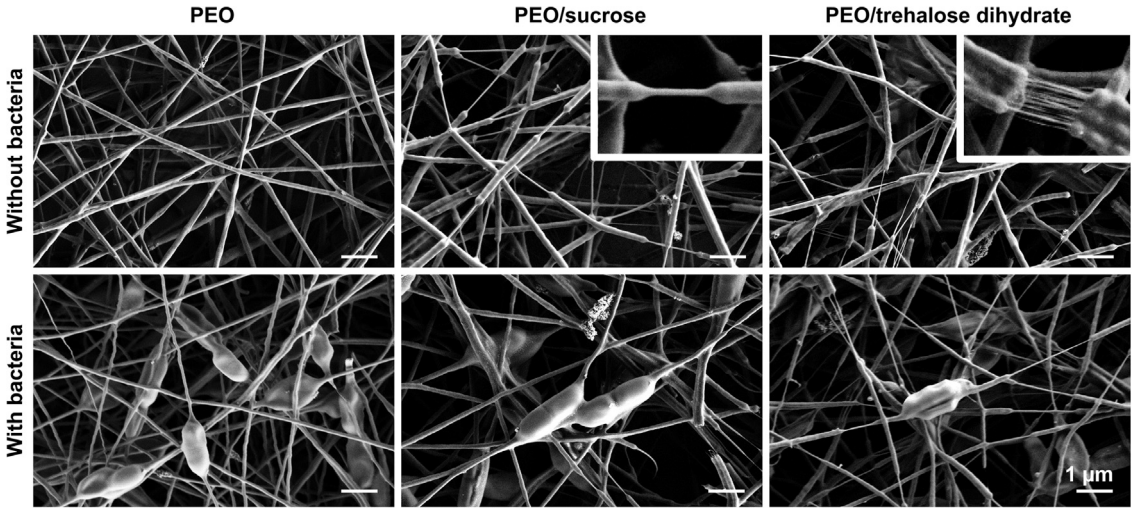

Fig. 3. Scanning electron microscopy images of poly(ethylene oxide) nanofibers without and with lyoprotectants (sucrose, trehalose dihydrate) and *L. plantarum* cells. Inserts show magnified images of the 'necks' in the nanofibers.

of ~15 nm were also seen in these neck regions, which were more frequent for the PEO/trehalose nanofibers. Indeed, some of the discontinued nanofibers that can be seen in Fig. 3 were created during the SEM examinations, where the 1 kV electronic beams broke these thin fibrils. Similar structures (i.e., necks) have been reported previously and were attributed to the strong stretching of the solidified PEO nanofibers that were collected on the tapered wheel at high rotation speeds [51,52]. This effect was promoted by increased ductility of the PEO/lyoprotectant nanofibers compared to those of pure PEO, which may be attributed to the changed solid state of the polymer due to the plasticiser effect of the lyoprotectant in the nanofibers.

3.3. Incorporation of L. plantarum into nanofibers reduces the crystallinity of the polymers and lyoprotectants

DSC was carried out to investigate the physical states of the nanofiber components and the possible interactions between them (Fig. 4, Table 1), and TGA was carried out to determine the moisture levels in the samples (Table 1). The thermograms of the dried *L. plantarum* cells (following lyophilization from water) showed two broad endothermic peaks at 100 °C and 196 °C (Fig. 4a). For the same temperatures, the decreases in the mass of the samples were determined by TGA. Consequently, the first peak shown in Fig. 4a represents evaporation of the water and the second probably represents degradation of some of the components of the *L. plantarum*. The moisture content of the lyophilized cells was 11% (Table 1). The pure PEO showed a sharp endothermic peak at 70.4 °C, which represents the melting temperature of the polymer (Fig. 4a). The sucrose and trehalose dihydrate melted at 193.7 °C (Fig. 4b) and 209.2 °C (Fig. 4c), respectively. Trehalose dihydrate also showed two additional peaks, at 100.9 °C and 121.1 °C, which were due to evaporation of the bound water. In the physical mixtures of PEO and the lyoprotectants, there were characteristic endothermic peaks for all of the components (Fig. 4b, c).

The electrospinning of the PEO solution decreased the crystallinity of PEO in the nanofibers, which was seen as the smaller endothermic peak and specific enthalpy of transition compared to pure PEO (Fig. 4a, Table 1). Similarly, in composite nanofibers, the electrospinning resulted in small to more pronounced reductions in the sucrose and trehalose crystallinities, respectively. Also, the presence of the *L. plantarum* cells in the nanofibers reduced the crystallinity of PEO and sucrose in the PEO and PEO/sucrose nanofibers (Fig. 4, Table 1). Moreover, addition of the *L. plantarum* cells to the PEO/trehalose nanofibers resulted in complete amorphization of the trehalose (Fig. 4c, Table 1). The shift in the PEO melting peak to lower temperatures in the nanofibers that contained *L. plantarum* cells, along with the reduced crystallinity of the sucrose and the amorphization of the trehalose, suggested interactions between PEO, lyoprotectants and the *L. plantarum* cells, as was similarly proposed previously for polymer blends [53]. The moisture content of the nanofibers with the *L. plantarum* cells was lower than that of the lyophilized *L. plantarum* cells (Table 1).

3.4. L. plantarum interacts with excipients in nanofibers

FTIR spectroscopy is a sensitive method to evaluate the interactions of excipients with proteins and polar head groups of lipid membranes in bacteria [54]. The *L. plantarum* cells lyophilized from water showed three main amide bands from proteins: amide A (3291 cm^{-1}), amide I (1651 cm^{-1}), and amide II (1529 cm^{-1}) (Fig. 5a). A peak at 1233 cm^{-1} can be attributed to amide III and/or phosphate asymmetric stretching vibrational mode, as both have been reported to be near to this wavenumber [54–56]. The symmetric and asymmetric CH_2 stretching vibrational modes of the lipid membranes were observed at 2862 cm^{-1} and 2928 cm^{-1}, respectively (Fig. 5a) [54].

To predict the effects of drying on bacterial proteins, the region of the amide I and amide II peaks at wavenumbers between 1500 cm^{-1} and 1700 cm^{-1} can be studied. Amide I represents C═O stretching vibration, and it can be used to assign the secondary structure of proteins. Amide II is composed of NH bending [55,56]. There were no peaks in this region in the spectra of the pure PEO, trehalose, and sucrose; their spectra thus do not overlap with the conformationally sensitive amide I and amide II peaks of *L. plantarum*. The amide I and amide II peaks from *L. plantarum*-loaded nanofibers are in good agreement with air-dried *L. plantarum* from the literature [56], at 1652 cm^{-1} and 1543 cm^{-1}, respectively. The amide I peak has a different shape for the lyophilized *L. plantarum* compared to the *L. plantarum*-loaded nanofibers (Fig. 5b). Similarly, the shape of the amide II peak was changed, as it had shifted from 1529 cm^{-1} (lyophilized *L. plantarum*) to 1543 cm^{-1} (*L. plantarum*-loaded nanofibers). Similar shifts in the amide II peak have been reported previously for protein lysozyme [57] and the bacteria *E. coli* and *Bacillus thuringiensis* comparing the hydrated cells (1543 cm^{-1}) to the cells dried without lyoprotectants (1533 cm^{-1}) [38]. The electrospinning without and with the added lyoprotectants might stabilize *L. plantarum* better than lyophilization in deionized water, as the decrease in vibrational frequency observed in the lyophilized *L. plantarum* represents a change in protein structure [38].

Hydrogen bonding between different excipients is often monitored in FTIR spectra by the hydroxyl stretching region between 3650 cm^{-1}

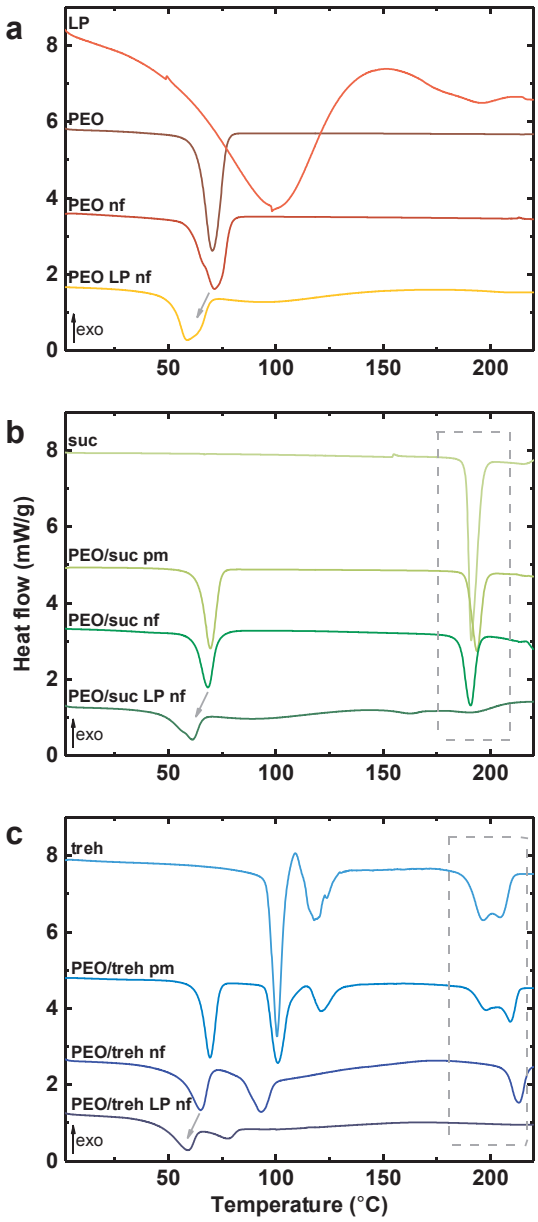

Fig. 4. Differential scanning calorimetry thermograms. **(a)** Lyophilized cells of *L. plantarum* (LP), pure poly(ethylene oxide) (PEO), PEO nanofibers (nf), and PEO nanofibers with *L. plantarum* (LP nf). **(b)** Sucrose (suc), physical mixture of PEO and sucrose (PEO/suc pm), PEO/sucrose nanofibers (PEO/suc nf), and PEO/sucrose nanofibers with *L. plantarum* (PEO/suc LP nf). **(c)** Trehalose dihydrate (treh), physical mixture of PEO and trehalose dihydrate (PEO/treh pm), PEO/trehalose nanofibers (PEO/treh nf), and PEO/trehalose nanofibers with *L. plantarum* (PEO/treh LP nf). The main changes in the spectra are marked with the dashed rectangles and arrows.

and 3100 cm^{-1} [57], which overlaps with the amide A region (NH stretching) at 3300 cm^{-1} [55]. Amide A is very sensitive to the strength of the hydrogen bonds and does not depend on the skeletal conformation [54]. In addition, the moisture in the samples affects the intensity of the amide A peak [58]. The PEO nanofibers did not have any peaks in this region, and so hydrogen bonds are not expected. For the *L. plantarum*-loaded PEO nanofibers, the peak at 3295 cm^{-1} was shifted from 3290 cm^{-1} in the lyophilized *L. plantarum* (Fig. 5c). The sucrose and trehalose dihydrate showed six sharp CH_2-stretching peaks between 2850 cm^{-1} and 3000 cm^{-1}, which were decreased in the PEO/sucrose and PEO/trehalose nanofibers and fused into one broad peak for the *L. plantarum*-loaded PEO/sucrose and PEO/trehalose nanofibers (Fig. 5c). Similarly, the peaks of sucrose and trehalose dihydrate with their characteristic shape at positions 3325 cm^{-1} and 3268 cm^{-1}, respectively, merged with the characteristic peak of the *L. plantarum* at 3290 cm^{-1} to form one broad peak, which was shifted to 3296 cm^{-1} for the *L. plantarum*-loaded PEO/sucrose nanofibers, and to 3287 cm^{-1} for the *L. plantarum*-loaded PEO/trehalose nanofibers (Fig. 5c). These changes in the spectra might be the consequence of hydrogen interactions between the lyoprotectants and the proteins of the *L. plantarum* cells, which correlates with the DSC data (Fig. 4). Although the shifts and changes in other regions of the FTIR spectra might provide additional information about interactions between the excipients and the *L. plantarum*, these are difficult to evaluate due to the extensive and intricate overlapping of the PEO, lyoprotectant, and *L. plantarum* peaks.

3.5. The process parameters and polymer solution compositions influence the viability of *L. plantarum* in electrospun nanofibers

The next challenge was to determine how variations in the electrospinning process and the environment and solution properties influenced the *L. plantarum* viability, and to define possible correlations of the components with the crystallinity, and interactions between the excipients and the *L. plantarum* cells. The high voltage applied in the electrospinning process is expected to be harmful to the *L. plantarum* cells, although it is necessary for the production of the nanofibers here [59]. Among the voltages investigated (10, 15, 20 kV), the *L. plantarum* cells showed their greatest viability at 15 kV (0.81 log reduction in viable *L. plantarum*, compared to theoretical *L. plantarum* loading) (Fig. 6a). Decreases in *L. plantarum* cell viability were seen both when the voltage was increased from 15 kV to 20 kV (2.03 log reduction in viable *L. plantarum*) and when the voltage was decreased from 15 kV to 10 kV (1.30 log reduction in viable *L. plantarum*). Additionally, electrospinning at 10 kV was less efficient than that at 15 kV and 20 kV, and resulted in lower nanofiber production per unit time. The relative humidity of 55% during the electrospinning resulted in higher cell viability (1.02 log reduction in viable *L. plantarum*, in comparison to theoretical *L. plantarum* loading) compared to 20% relative humidity (1.81 log reduction in viable *L. plantarum*).

The *L. plantarum* concentrations in the PEO solution were the most critical parameter for their viability when incorporated into the nanofibers (Fig. 6b). Contrary to the number of *L. plantarum* cells incorporated when observed by SEM, the number of viable *L. plantarum* cells in the nanofibers did not correlate with the number of *L. plantarum* cells in the polymer solutions. Here, a 10-fold decrease in the concentration of *L. plantarum* cells in the polymer solution did not result in a 10-fold decrease in their viability, but rather, a 1000-fold decrease. The use of the polymer solutions with 12 log CFU/mL *L. plantarum* cells (i.e., the highest concentration used here) resulted in 1.18 log decrease in viable *L. plantarum* cells (from the theoretical yield of 10.06 log to 8.88 log CFU/mg). A 10-fold decrease in the *L. plantarum* concentration (11 log CFU/mL) resulted in a 3.73 log decrease in viability (from the theoretical 9.39 to 5.66 log CFU/mg), and a 100-fold decrease in the *L. plantarum* concentration (10 log CFU/mL) resulted in a 5.99 log decrease in viability (from the theoretical 8.47 to 2.48 log CFU/mg of viable *L. plantarum* cells), while with a 1000-fold decrease in the *L. plantarum* concentration (9 log CFU/mL) there were no viable *L. plantarum* cells in the nanofibers. However, at the highest investigated concentration of *L. plantarum*, the number of viable *L. plantarum* cells in the nanofibers almost reached the theoretical number of *L. plantarum* cells incorporated. This importance of the initial concentration of the *L. plantarum* (i.e., prior to drying) for their survival has not been reported previously for electrospinning, although it has been seen for lyophilization [60,61]. This was attributed to the mutual shielding effects of the bacteria and their decreased exposure to the detrimental conditions of the medium, due to the smaller contact area when the bacteria are at high concentrations [62]. For *L. plantarum*, highly concentrated bacterial dispersions should thus be used for electrospinning, to decrease

Table 1
PEO and lyoprotectant endothermic peaks and moisture content of the PEO nanofibers without and with the *L. plantarum* cells. The theoretical enthalpy for the PEO and lyoprotectants represents the enthalpy of crystalline substances with respect to their percentages in the nanofibers.

Sample	PEO melting			Lyoprotectant melting			Moisture content (%)
	Theoretical enthalpy (J/g)	Enthalpy (J/g)	Peak (°C)	Theoretical enthalpy (J/g)	Enthalpy (J/g)	Peak (°C)	
Lyophilized *L. plantarum*	/	/	/	/	/	/	10.8
PEO	/	−170.2	70.42	/	/	/	< 1.5
PEO nanofibers	−170.2	−141.4	71.51	/	/	/	< 1.5
L. plantarum-loaded PEO nanofibers	−102.1	−89.3	58.83	/	/	/	5.3
Sucrose	/	/	/	/	−133.4	190.9	< 1.5
PEO/sucrose physical mixture (1:1, w/w)	−85.1	−89.2	69.59	−66.7	−67.1	193.7	< 1.5
PEO/sucrose nanofibers	−85.1	−69.6	68.38	−66.7	−63.8	190.8	< 1.5
L. plantarum-loaded PEO/sucrose nanofibers	−67.0	−42.6	61.10	−52.6	−42.9	191.6	5.2
Trehalose	/	/	/	/	−121.6	196.5	9.6
PEO/trehalose physical mixture (1:1, w/w)	−78.3	−79.9	69.44	−61.4	−72.5	209.2	5.8
PEO/trehalose nanofibers	−80.1	−69.2	64.92	−62.8	−40.0	213.1	5.8
L. plantarum-loaded PEO/trehalose nanofibers	−66.7	−35.9	58.92	−52.3	−0.9	209.9	6.6

PEO, poly(ethylene oxide).

the influence of this process on the *L. plantarum* viability. As well as the concentration of bacteria, the growth phase of bacteria has also been reported to influence bacterial survival [63]. Harvesting of the bacteria in the early stationary phase has more frequently been reported as optimal, compared to harvesting in the late exponential phase. The early stationary phase has been shown to provide better bacterial survival during drying [16], and this was therefore adopted in the present study (i.e., harvesting at 12 h after inoculation).

The two lyoprotectants used in the present study provided similar levels of *L. plantarum* cell protection during the electrospinning for the composite nanofibers with PEO and lyoprotectant (1:1, w/w). In more detail, the addition of sucrose or trehalose dihydrate to the PEO nanofibers resulted in lower decrease in *L. plantarum* cell viability compared to the PEO nanofibers without these lyoprotectants in respect to theoretical loading of *L. plantarum* in individual formulation. For the PEO/sucrose and PEO/trehalose nanofibers, only 0.74 log and 0.80 log reductions in *L. plantarum* cell viability was determined, respectively, whereas in the absence of lyoprotectants, cell viability was reduced by 1.21 log unit. As reported, the loss of viability during electrospinning can be caused by rapid evaporation of water and drastic change in the osmotic environment during drying. The bacterial membrane is the most common site of damage, because of the loss of water from both the lipid bilayer and the membrane proteins [64]. According to the water replacement hypothesis, lyoprotectants can substitute for the water molecules during drying by forming hydrogen bonds around the polar and charged groups in the phospholipid membranes and proteins, and thereby stabilize the native structure in the absence of water [17,18]. The formation of interactions between the lyoprotectants and the *L. plantarum* cells, and the amorphous state of trehalose in the nanofibers shown in the present study (Figs. 4, 5), will have important contributions to the improved *L. plantarum* cell viability during the electrospinning.

3.6. Viability of L. plantarum in nanofibers and in lyophilizates during storage

High viability of bacteria immediately after electrospinning is important; however, it is even more vital to maintain the viability during long-term storage. In our preliminary studies, the storage of PEO nanofibers at 25 °C without control of the relative humidity resulted in total loss of bacterial viability after 4 weeks. Given the large surface area of the nanofibers, ambient conditions such as heat and humidity might indeed be detrimental during storage of the bacteria incorporated into the nanofibers. Thus, the effects of the lyoprotectants (i.e., sucrose, trehalose) and temperature (4 °C, 25 °C) on the viability of the *L. plantarum* cells in the nanofibers were investigated here for a storage period of 24 weeks under controlled conditions at constant relative humidity of 11% (Fig. 7).

The viability of the *L. plantarum* cells in the PEO nanofibers at 25 °C was quickly reduced by more than 2 log units after 1 week, and by almost 4 log units after 12 weeks, with complete loss of viability after 24 weeks. The survival of the *L. plantarum* cells was improved in the PEO/sucrose nanofibers (3.8 log reduction after 24 weeks), while the PEO/trehalose nanofibers provided the highest viability at 25 °C (1.8 log reduction after 24 weeks). The stabilizing effects of these disaccharides for the *L. plantarum* cells are in line with previous studies of freeze-drying of such bacterial probiotics [65]. The improved *L. plantarum* viability for the PEO/trehalose nanofibers compared to that with PEO/sucrose might be the consequence of the amorphous state of trehalose, which can interact with and stabilize the bacterial membrane, compared to the partially crystalline state of sucrose. The moisture content retained in these nanofibers after their preparation (6% to 8%; Table 1) was also in line with previous reports [66,67], which suggests that the determined moisture content is optimal for preservation of high probiotic bacteria viability during storage.

The *L. plantarum* cells in the nanofibers stored at 4 °C for 24 weeks showed greater viability compared to those stored at 25 °C, while the *L. plantarum* cell viability in the nanofibers with added trehalose decreased by only 0.2 log units after 24 weeks of storage. The sucrose again showed less protection of the *L. plantarum* cells (0.5 log reduction), although their stability in these sucrose nanofibers was still better than for the PEO nanofibers without the lyoprotectants (0.8 log reduction). Beneficial effects of trehalose addition on the storage of nanofibers was demonstrated previously for bacteriophage T7, where the inclusion of trehalose also had no detrimental effects on the electrospinning process [49]. Generally, it has been well established that storage at lower temperatures can increase the survival of the bacteria [15], which was also shown in present study. Better survival of bacteria during long-term storage at lower temperatures is the consequence of the slowed bacterial metabolism [68]. On the other hand, the difference in the stability of such samples at 2–8 °C and at –20 °C is very small, and thus freezing is not necessary [36].

In contrast to electrospinning, lyophilization is a well-established method for preservation and storage of probiotics for industrial

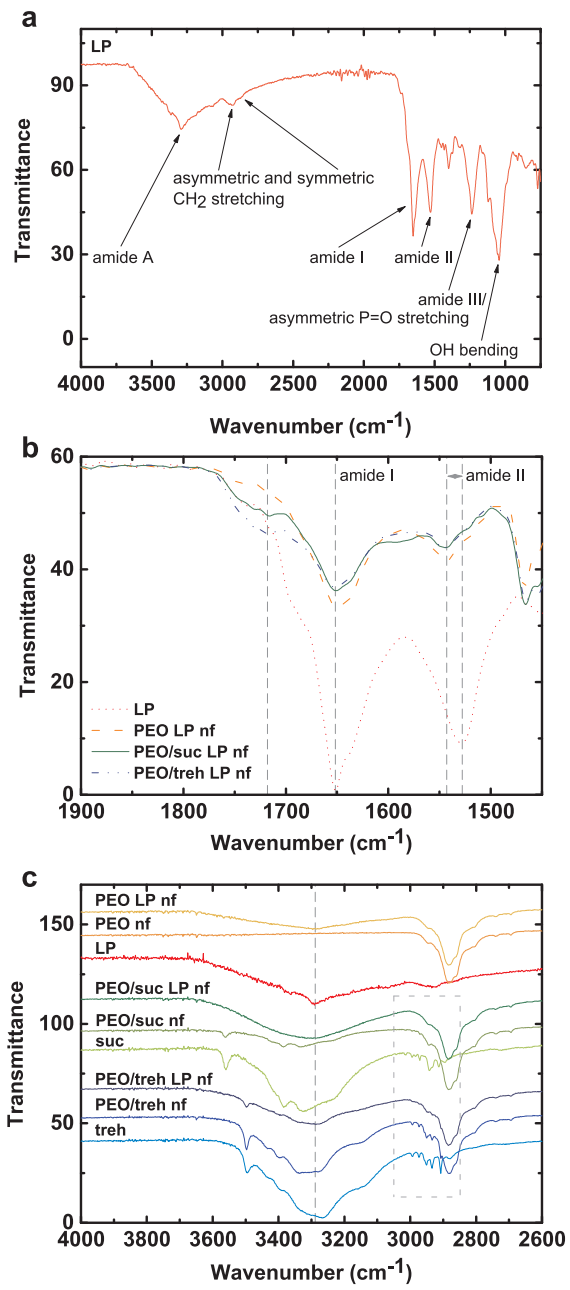

Fig. 5. Fourier transform infrared spectra. **(a)** Whole spectrum of lyophilized *L. plantarum* (LP). **(b)** Amide band region of lyophilized *L. plantarum* (LP) and *L. plantarum*-loaded poly(ethylene oxide) nanofibers (PEO nf) without and with addition of sucrose (suc) and trehalose (treh). **(c)** Amide A stretching region of lyophilized *L. plantarum* (LP), pure sucrose (suc) and trehalose dehydrate (treh), and all of the prepared nanofibers (without and with lyoprotectants, without and with *L. plantarum*, as indicated). The main changes in the spectra are indicated by the dashed lines and rectangles.

applications [69]. The survival rates of *L. plantarum* following electrospinning and lyophilization were thus also compared here (Fig. 7). At 25 °C, the viability of the *L. plantarum* cells in the lyophilized samples prepared from *L. plantarum* cell dispersions in 4% (w/v) PEO solution without added lyoprotectants decreased by 4.0 log units over 24 weeks. For the nanofibers with a similar composition, no viable bacteria were detected after this time. The addition of sucrose to the *L. plantarum* dispersions increased their survival in lyophilized samples in comparison to samples without sucrose over 24 weeks (1.70 log decrease in viability, from 9.07 to 7.37 CFU/mg). However, the inclusion of sucrose in the nanofibers was less efficient, as it resulted in a 3.8 log decrease in *L. plantarum* cell viability over 24 weeks (from 8.04 to 4.17 CFU/mg). Instead, the addition of trehalose to the nanofibers was the most effective for the viability of the *L. plantarum* cells, regardless of the drying technique used (i.e., lyophilization, electrospinning). Here, there were no significant differences for the *L. plantarum* cell survival between lyophilization and electrospinning, with 24 weeks of storage at 25 °C resulting in 1.70 log units (from 8.97 to 7.27 CFU/mg) and 1.83 log units (from 8.51 to 6.68 CFU/mg) decreases, respectively. Storage at 4 °C resulted in significantly higher *L. plantarum* cell viability in comparison to storage at 25 °C, regardless of whether lyophilization or electrospinning were used for the drying. Also, at 4 °C, the differences in the *L. plantarum* cell viabilities across lyophilization and electrospinning were minimal. These data indicate that storage at low temperatures and addition of lyoprotectants, and especially trehalose, represent good strategies to extend the shelf-life of such probiotic products, which is in agreement with the literature [70]. Under such conditions, the survival of bacteria in such lyophilized and electrospun products with similar compositions is comparable.

3.7. Release of *L. plantarum* from nanofibers

After storage, the viable probiotics need to be delivered to the local site of the disease, to be available for recolonization of the niche. Nanofibers made with mucoadhesive polymer PEO should offer a promising delivery system for their adherence to the mucosa. In the release study performed here in PBS (Fig. 8), near total release of the *L. plantarum* cells from the nanofibers was achieved within the first 30 min (> 90%). This was seen by both methods used: CFU determination, and fluorescence measurements of the mCherry protein constitutively expressed in the cytoplasm of the *L. plantarum* cells, whereby the fluorescence was representative of the *L. plantarum* cell concentration [40]. This release over 30 min might represent sufficient time for the probiotic bacteria to attach to the surface of the mucosa, and thus prevent their immediate flushing with body fluids. On the other hand, the dissolution of the PEO nanofiber mat over 30 min is also beneficial for the rapid removal of the delivery system from the body. *L. plantarum* cells that express fluorescent mCherry protein can be incorporated into nanofibers and used to monitor their release, and thus to track the fate of these bacteria *in vivo* in experimental animals, as we have reported previously [71].

4. Conclusions

In the present study, we successfully developed monolithic PEO and composite PEO/lyoprotectant nanofibers that provided high loading of *L. plantarum* cells (up to 7.6×10^8 CFU/mg). The most critical parameter for high *L. plantarum* cell viability after the electrospinning was the concentration of these probiotic *L. plantarum* cells in the PEO solution, whereas the applied voltage and the relative humidity during the electrospinning did not have any vital impact on *L. plantarum* cell viability. The addition of high contents of lyoprotectants, and especially trehalose, to the composite nanofibers (PEO:lyoprotectant, 1:1 (w/w)) provided small improvements in the *L. plantarum* cell viabilities after the electrospinning, but large survival benefits during storage. The minimal loss of the *L. plantarum* cell viability over 24 weeks of storage at low temperature can also be attributed to the amorphous state of the trehalose interacting with the *L. plantarum* cells. The PEO nanofibers released almost all of the *L. plantarum* cells over 30 min, which will be appropriate for their local administration. The present study also included the first incorporation into nanofibers of recombinant probiotic bacteria that were expressing a fluorescent protein, which will facilitate *in vivo* studies by providing a simple tracking method for these probiotics, to thus promote deeper understanding of such treatments. In summary, this approach demonstrates the development of a promising local nanodelivery system based on the use of probiotic-loaded nanofibers that can provide high loading and long shelf life. Such delivery

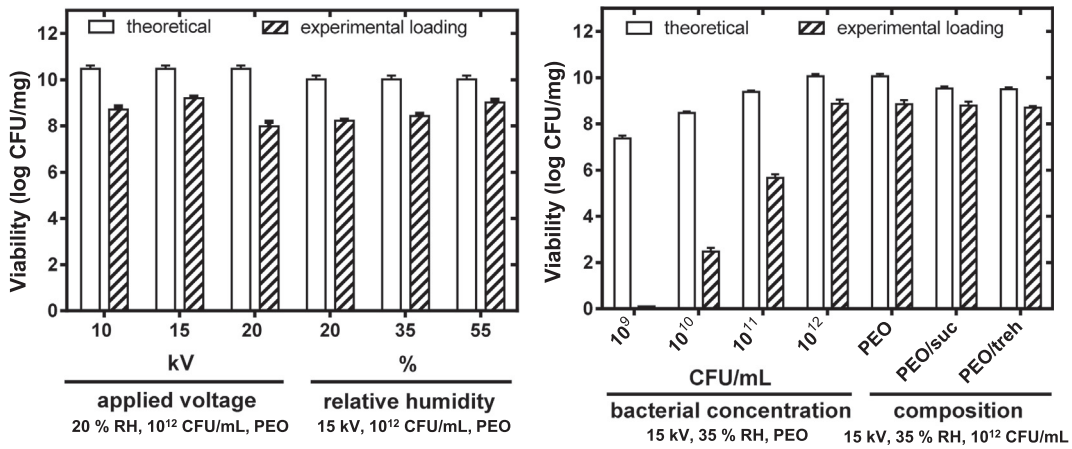

Fig. 6. Effects of the process and environmental parameters (voltage, relative humidity) (**a**) and the properties of the poly(ethylene oxide) (PEO) dispersion (*L. plantarum* concentration, lyoprotectants) (**b**) on viability of the *L. plantarum* cells at 24 h after the electrospinning, in terms of the theoretical and experimentally determined viable *L. plantarum* loading.

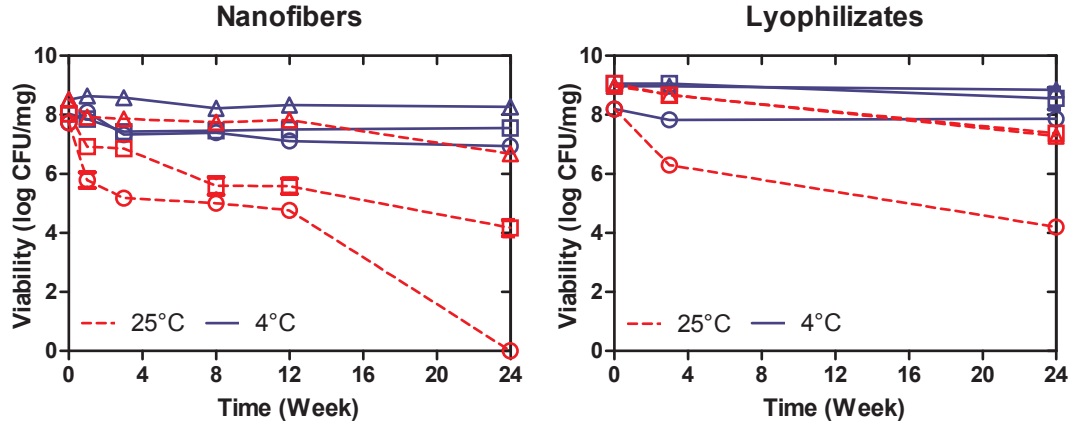

Fig. 7. Viability of *L. plantarum* cells in nanofibers and lyophilizates obtained from poly(ethylene oxide) (PEO; circles), PEO/sucrose (squares), and PEO/trehalose (triangles) solutions. The samples were stored at 11% relative humidity, at 25 °C (red) or 4 °C (blue).

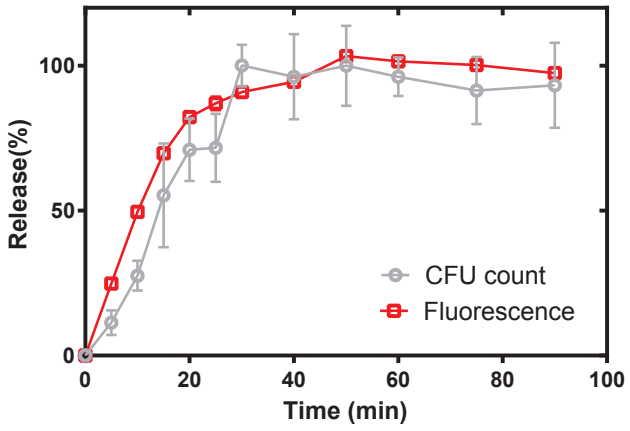

Fig. 8. Release of *L. plantarum* cells from poly(ethylene oxide) (PEO) nanofibers determined by CFU counting (circle) and by measuring the fluorescence of the mCherry protein (square). The *L. plantarum* cell release (%) was determined as the proportion of the CFU and fluorescence measures relative to the final CFU count (2.07×10^9 CFU) and fluorescence (3.85×10^6 fluorescence units), respectively.

system could be particularly useful for the vaginal delivery of different *Lactobacillus* species.

5. Declarations of interest

None.

Acknowledgements

This study was supported by the Slovenian Research Agency (grant numbers P4-0127, P1-0189 and J1-9194). We thank Dr Christopher Berrie for critical reading of the manuscript, and Dr Stefan Heinl for providing plasmid pCDLbu-1ΔEc_Ptuf34_mCherry.

References

[1] S. Carding, K. Verbeke, D.T. Vipond, B.M. Corfe, L.J. Owen, Dysbiosis of the gut microbiota in disease, Microb. Ecol. Health Dis. 26 (2015) 26191.
[2] C.P. Tamboli, C. Neut, P. Desreumaux, J.F. Colombel, Dysbiosis in inflammatory bowel disease, Gut 53 (2004) 1–4.
[3] P.J. Kennedy, J.F. Cryan, T.G. Dinan, G. Clarke, Irritable bowel syndrome: a microbiome-gut-brain axis disorder? World J. Gastroenterol. 20 (2014) 14105–14125.
[4] J.H.H.M. van de Wijgert, V. Jespers, The global health impact of vaginal dysbiosis, Res. Microbiol. 168 (2017) 859–864.
[5] S. Zupancic, P. Kocbek, S. Baumgartner, J. Kristl, Contribution of nanotechnology to improved treatment of periodontal disease, Curr. Pharm. Des. 21 (2015) 3257–3271.
[6] Y.E. Chen, H. Tsao, The skin microbiome: current perspectives and future challenges, J. Am. Acad. Dermatol. 69 (2013) 143–155.

[7] C. Hill, F. Guarner, G. Reid, G.R. Gibson, D.J. Merenstein, B. Pot, L. Morelli, R.B. Canani, H.J. Flint, S. Salminen, P.C. Calder, M.E. Sanders, The International Scientific Association for Probiotics and Prebiotics consensus statement on the scope and appropriate use of the term probiotic, Nat. Rev. Gastroenterol. Hepatol. 11 (2014) 506.
[8] C.A. Batt, Lactobacillus, in: C.A. Batt, M.L. Tortorello (Eds.), Encyclopedia of food microbiology, Academic Press, New York, USA, 2014, pp. 409–411.
[9] M. Cammarota, M. De Rosa, A. Stellavato, M. Lamberti, I. Marzaioli, M. Giuliano, *In vitro* evaluation of *Lactobacillus plantarum* DSMZ 12028 as a probiotic: Emphasis on innate immunity, Int. J. Food Microbiol. 135 (2009) 90–98.
[10] P. Ducrotte, P. Sawant, V. Jayanthi, Clinical trial: *Lactobacillus plantarum* 299v (DSM 9843) improves symptoms of irritable bowel syndrome, World J. Gastroenterol. 18 (2012) 4012–4018.
[11] M. Schultz, C. Veltkamp, L.A. Dieleman, W.B. Grenther, P.B. Wyrick, S.L. Tonkonogy, R.B. Sartor, *Lactobacillus plantarum* 299V in the treatment and prevention of spontaneous colitis in interleukin-10-deficient mice, Inflamm. Bowel Dis. 8 (2002) 71–80.
[12] M.C. de Vries, E.E. Vaughan, M. Kleerebezem, W.M. de Vos, *Lactobacillus plantarum*—survival, functional and potential probiotic properties in the human intestinal tract, Int. Dairy J. 16 (2006) 1018–1028.
[13] L. Satish, P.H. Gallo, S. Johnson, C.C. Yates, S. Kathju, Local probiotic therapy with *Lactobacillus plantarum* mitigates scar formation in rabbits after burn injury and infection, Surg. Infect. (Larchmt) 18 (2017) 119–127.
[14] J.M. Wells, A. Mercenier, Mucosal delivery of therapeutic and prophylactic molecules using lactic acid bacteria, Nat. Rev. Microbiol. 6 (2008) 349.
[15] G. Broeckx, D. Vandenheuvel, I.J.J. Claes, S. Lebeer, F. Kiekens, Drying techniques of probiotic bacteria as an important step towards the development of novel pharmabiotics, Int. J. Pharm. 505 (2016) 303–318.
[16] J. Mirtic, T. Rijavec, S. Zupancic, A. Zvonar Pobirk, A. Lapanje, J. Kristl, Development of probiotic-loaded microcapsules for local delivery: Physical properties, cell release and growth, Eur. J. Pharm. Sci. 121 (2018) 178–187.
[17] J.H. Crowe, L.M. Crowe, D. Chapman, Preservation of membranes in anhydrobiotic organisms: the role of trehalose, Science 223 (1984) 701–703.
[18] L.M. Crowe, D.S. Reid, J.H. Crowe, Is trehalose special for preserving dry biomaterials? Biophys. J. 71 (1996) 2087–2093.
[19] C.C. Coghetto, G.B. Brinques, M.A. Ayub, Probiotics production and alternative encapsulation methodologies to improve their viabilities under adverse environmental conditions, Int. J. Food Sci. Nutr. 67 (2016) 929–943.
[20] I. Wagner, Z.K. Nagy, Á. Suhajda, H. Pataki, P. Sóti, T. Vigh, A. Balogh, A.H. Harasztos, G. Marosi, Film coating as a new approach to prepare tablets containing long-term stable *Lactobacillus acidophilus*, Period. Polytech. Chem. 59 (2015) 96–103.
[21] Š. Zupančič, T. Rijavec, A. Lapanje, M. Petelin, J. Kristl, P. Kocbek, Nanofibers with incorporated autochthonous bacteria as potential probiotics for local treatment of periodontal disease, Biomacromolecules 19 (2018) 4299–4306.
[22] N.O. San Keskin, A. Celebioglu, O.F. Sarioglu, T. Uyar, T. Tekinay, Encapsulation of living bacteria in electrospun cyclodextrin ultrathin fibers for bioremediation of heavy metals and reactive dye from wastewater, Colloids Surf. B Biointerf. 161 (2018) 169–176.
[23] P. Jun-Seo, Electrospinning and its applications, Adv. Nat. Sci. Nanosci. Nanotechnol. 1 (2010) 043002.
[24] H.P. Felgueiras, M.T.P. Amorim, Functionalization of electrospun polymeric wound dressings with antimicrobial peptides, Colloids Surf. B Biointerf. 156 (2017) 133–148.
[25] R. Rosic, P. Kocbek, J. Pelipenko, J. Kristl, S. Baumgartner, Nanofibers and their biomedical use, Acta Pharm. 63 (2013) 295–304.
[26] E.A. Krogstad, R. Ramanathan, C. Nhan, J.C. Kraft, A.K. Blakney, S. Cao, R.J.Y. Ho, K.A. Woodrow, Nanoparticle-releasing nanofiber composites for enhanced *in vivo* vaginal retention, Biomaterial 144 (2017) 1–16.
[27] F. Brako, B. Raimi-Abraham, S. Mahalingam, D.Q.M. Craig, M. Edirisinghe, Making nanofibres of mucoadhesive polymer blends for vaginal therapies, Eur. Polym. J. 70 (2015) 186–196.
[28] S. Zupancic, L. Preem, J. Kristl, M. Putrins, T. Tenson, P. Kocbek, K. Kogermann, Impact of PCL nanofiber mat structural properties on hydrophilic drug release and antibacterial activity on periodontal pathogens, Eur. J. Pharm. Sci. 122 (2018) 347–358.
[29] X. Hu, S. Liu, G. Zhou, Y. Huang, Z. Xie, X. Jing, Electrospinning of polymeric nanofibers for drug delivery applications, J. Contr. Rel. 185 (2014) 12–21.
[30] K. Khoshnevisan, H. Maleki, H. Samadian, S. Shahsavari, M.H. Sarrafzadeh, B. Larijani, F.A. Dorkoosh, V. Haghpanah, M.R. Khorramizadeh, Cellulose acetate electrospun nanofibers for drug delivery systems: Applications and recent advances, Carbohydr. Polym. 198 (2018) 131–141.
[31] I. Wagner, Z.K. Nagy, P. Vass, C. Fehér, Z. Barta, T. Vigh, P.L. Sóti, A.H. Harasztos, H. Pataki, A. Balogh, G. Verreck, I.V. Assche, G. Marosi, Stable formulation of protein-type drug in electrospun polymeric fiber followed by tableting and scaling-up experiments, Polym. Adv. Technol. 26 (2015) 1461–1467.
[32] Z.-M. Huang, Y.Z. Zhang, M. Kotaki, S. Ramakrishna, A review on polymer nanofibers by electrospinning and their applications in nanocomposites, Compos. Sci. Technol. 63 (2003) 2223–2253.
[33] W.Y. Fung, K.H. Yuen, M.T. Liong, Agrowaste-based nanofibers as a probiotic encapsulant: fabrication and characterization, J. Agric. Food Chem. 59 (2011) 8140–8147.
[34] A. Lopez-Rubio, E. Sanchez, Y. Sanz, J.M. Lagaron, Encapsulation of living bifidobacteria in ultrathin PVOH electrospun fibers, Biomacromolecules 10 (2009) 2823–2829.
[35] W. Salalha, J. Kuhn, Y. Dror, E. Zussman, Encapsulation of bacteria and viruses in electrospun nanofibres, Nanotechnology 17 (2006) 4675.
[36] Z.K. Nagy, I. Wagner, Á. Suhajda, T. Tobak, A. Harasztos, T. Vigh, P. Soti, H. Pataki, K. Molnar, G. Marosi, Nanofibrous solid dosage form of living bacteria prepared by electrospinning, Express Polym. Lett. 8 (2014) 352–361.
[37] K. Knop, R. Hoogenboom, D. Fischer, S. Schubert Ulrich, Poly(ethylene glycol) in drug delivery: pros and cons as well as potential alternatives, Angew. Chem. Int. Ed. 49 (2010) 6288–6308.
[38] S.B. Leslie, E. Israeli, B. Lighthart, J.H. Crowe, L.M. Crowe, Trehalose and sucrose protect both membranes and proteins in intact bacteria during drying, Appl. Environ. Microbiol. 61 (1995) 3592–3597.
[39] F. Berthier, M. Zagorec, M. Champomier-Vergès, S.D. Ehrlich, F. Morel-Deville, Efficient transformation of *Lactobacillus sake* by electroporation, Microbiology 142 (1996) 1273–1279.
[40] C. Tauer, S. Heinl, E. Egger, S. Heiss, R. Grabherr, Tuning constitutive recombinant gene expression in *Lactobacillus plantarum*, Microb. Cell Fact. 13 (2014) 150.
[41] B. Herigstad, M. Hamilton, J. Heersink, How to optimize the drop plate method for enumerating bacteria, J. Microbiol. Meth. 44 (2001) 121–129.
[42] W. Salalha, Y. Dror, R.L. Khalfin, Y. Cohen, A.L. Yarin, E. Zussman, Single-walled carbon nanotubes embedded in oriented polymeric nanofibers by electrospinning, Langmuir 20 (2004) 9852–9855.
[43] S.N. Reznik, A.L. Yarin, E. Zussman, L. Bercovici, Evolution of a compound droplet attached to a core-shell nozzle under the action of a strong electric field, Phys. Fluids 18 (2006) 062101.
[44] J. Pelipenko, P. Kocbek, J. Kristl, Critical attributes of nanofibers: preparation, drug loading, and tissue regeneration, Int. J. Pharm. 484 (2015) 57–74.
[45] V. Beachley, X. Wen, Effect of electrospinning parameters on the nanofiber diameter and length, Mater. Sci. Eng. C Mater. Biol. Appl. 29 (2009) 663–668.
[46] J. Pelipenko, J. Kristl, B. Jankovic, S. Baumgartner, P. Kocbek, The impact of relative humidity during electrospinning on the morphology and mechanical properties of nanofibers, Int. J. Pharm. 456 (2013) 125–134.
[47] C.J. Thompson, G.G. Chase, A.L. Yarin, D.H. Reneker, Effects of parameters on nanofiber diameter determined from electrospinning model, Polymer (Guildf) 48 (2007) 6913–6922.
[48] P. Gupta, C. Elkins, T.E. Long, G.L. Wilkes, Electrospinning of linear homopolymers of poly(methyl methacrylate): exploring relationships between fiber formation, viscosity, molecular weight and concentration in a good solvent, Polymer (Guildf) 46 (2005) 4799–4810.
[49] M. Dai, A. Senecal, S.R. Nugen, Electrospun water-soluble polymer nanofibers for the dehydration and storage of sensitive reagents, Nanotechnology 25 (2014) 225101.
[50] C.K. Koo, K. Senecal, A. Senecal, S.R. Nugen, Dehydration of bacteriophages in electrospun nanofibers: effect of excipients in polymeric solutions, Nanotechnology 27 (2016) 485102.
[51] E. Zussman, D. Rittel, A.L. Yarin, Failure modes of electrospun nanofibers, Appl. Phys. Lett. 82 (2003) 3958–3960.
[52] S. Tungprapa, I. Jangchud, P. Ngamdee, M. Rutnakornpituk, P. Supaphol, Ultrafine electrospun poly(ethylene glycol)–polydimethylsiloxane–poly(ethylene glycol) triblock copolymer/poly(ethylene oxide) blend fibers, Mater. Lett. 60 (2006) 2920–2924.
[53] P. Xing, L. Dong, Y. An, Z. Feng, M. Avella, E. Martuscelli, Miscibility and crystallization of poly(β-hydroxybutyrate) and poly(p-vinylphenol) blends, Macromolecules 30 (1997) 2726–2733.
[54] M.I. Santos, E. Gerbino, E. Tymczyszyn, A. Gomez-Zavaglia, Applications of infrared and raman spectroscopies to probiotic investigation, Foods 4 (2015) 283–305.
[55] J. Kong, S. Yu, Fourier transform infrared spectroscopic analysis of protein secondary structures, Acta Biochim. Biophys. Sin. (Shanghai) 39 (2007) 549–559.
[56] L.J. Linders, W.F. Wolkers, F.A. Hoekstra, K. van 't Riet, Effect of added carbohydrates on membrane phase behavior and survival of dried *Lactobacillus plantarum*, Cryobiology 35 (1997) 31–40.
[57] J.F. Carpenter, J.H. Crowe, An infrared spectroscopic study of the interactions of carbohydrates with dried proteins, Biochemistry 28 (1989) 3916–3922.
[58] J.M. Vanderkooi, J.L. Dashnau, B. Zelent, Temperature excursion infrared (TEIR) spectroscopy used to study hydrogen bonding between water and biomolecules, Biochim. Biophys. Acta Proteins Proteom. 1749 (2005) 214–233.
[59] Y. Liu, M.H. Rafailovich, R. Malal, D. Cohn, D. Chidambaram, Engineering of biohybrid materials by electrospinning polymer-microbe fibers, Proc. Natl. Acad. Sci. USA 106 (2009) 14201–14206.
[60] E. Costa, J. Usall, N. Teixido, N. Garcia, I. Vinas, Effect of protective agents, rehydration media and initial cell concentration on viability of *Pantoea agglomerans* strain CPA-2 subjected to freeze-drying, J. Appl. Microbiol. 89 (2000) 793–800.
[61] J. Palmfeldt, P. Radstrom, B. Hahn-Hagerdal, Optimisation of initial cell concentration enhances freeze-drying tolerance of *Pseudomonas chlororaphis*, Cryobiology 47 (2003) 21–29.
[62] T.F. Bozoğlu, M. Özilgen, U. Bakir, Survival kinetics of lactic acid starter cultures during and after freeze drying, Enzyme Microb. Technol. 9 (1987) 531–537.
[63] S.H. Peighambardoust, A. Golshan Tafti, J. Hesari, Application of spray drying for preservation of lactic acid starter cultures: a review, Trends Food Sci. Technol. 22 (2011) 215–224.
[64] R. Korehei, J. Kadla, Incorporation of T4 bacteriophage in electrospun fibres, J. Appl. Microbiol. 114 (2013) 1425–1434.
[65] S. Miao, S. Mills, C. Stanton, G.F. Fitzgerald, Y. Roos, R.P. Ross, Effect of disaccharides on survival during storage of freeze dried probiotics, Dairy Sci. Technol. 88 (2008) 19–30.
[66] G. Zayed, Y.H. Roos, Influence of trehalose and moisture content on survival of *Lactobacillus salivarius* subjected to freeze-drying and storage, Process Biochem. 39 (2004) 1081–1086.

[67] S.C. Zhu, D.Y. Ying, L. Sanguansri, J.W. Tang, M.A. Augustin, Both stereo-isomers of glucose enhance the survival rate of microencapsulated *Lactobacillus rhamnosus* GG during storage in the dry state, J. Food Eng. 116 (2013) 809–813.
[68] G. Broeckx, D. Vandenheuvel, T. Henkens, S. Kiekens, M.F.L. van den Broek, S. Lebeer, F. Kiekens, Enhancing the viability of *Lactobacillus rhamnosus* GG after spray drying and during storage, Int. J. Pharm. 534 (2017) 35–41.
[69] B. Li, F. Tian, X. Liu, J. Zhao, H. Zhang, W. Chen, Effects of cryoprotectants on viability of *Lactobacillus reuteri* CICC6226, Appl. Microbiol. Biotechnol. 92 (2011) 609–616.
[70] J. Agudelo, A. Cano, C. González-Martínez, A. Chiralt, Disaccharide incorporation to improve survival during storage of spray dried *Lactobacillus rhamnosus* in whey protein-maltodextrin carriers, J. Funct. Food. 37 (2017) 416–423.
[71] A. Berlec, J. Zavrsnik, M. Butinar, B. Turk, B. Strukelj, *In vivo* imaging of *Lactococcus lactis*, *Lactobacillus plantarum* and *Escherichia coli* expressing infrared fluorescent protein in mice, Microb. Cell Fact. 14 (2015) 181.